Coexistence of directed momentum current and ballistic energy diffusion in coupled non-Hermitian kicked rotors

Jian-Zheng Li [ORCID],[1] Wen-Lei Zhao [ORCID],[1,*] and Jie Liu [ORCID][2,3,†]

[1]*School of Science, Jiangxi University of Science and Technology, Ganzhou 341000, China*
[2]*Graduate School, China Academy of Engineering Physics, Beijing 100193, China*
[3]*HEDPS, Center for Applied Physics and Technology, and College of Engineering, Peking University, Beijing 100871, China*

We numerically investigate the quantum transport in coupled kicked rotors with $\mathcal{PT}$-symmetric potential. We find that spontaneous $\mathcal{PT}$-symmetry breaking of wave functions emerges when the amplitude of the imaginary part of the complex potential is beyond a threshold value, which can be modulated by the coupling strength effectively. In the regime of $\mathcal{PT}$-symmetry breaking, the particles driven by the periodical kicks move unidirectionally in momentum space, indicating the emergence of a directed current. Meanwhile, with increasing the coupling strength, we find a transition from the ballistic energy diffusion to a kind of modified ballistic energy diffusion where the width of the wave packet also increases with time in a power law. Our findings suggest that the decoherence effect induced by the interplay between the interparticle coupling and the non-Hermitian driving potential is responsible for these particular transport behaviors.

I. INTRODUCTION

Directed transport and quantum diffusion in both real and momentum space have attracted much interest in diverse fields of physics, ranging from condensed matter physics [1] to quantum chaos [2,3] and biological physics [4]. It is found that a seminal phenomenon of directed transport, namely, quantum ratchet [5], has practical applications in the design of electron pumps [6], in enhancing the efficiency of photovoltaic cells [7], and in the construction of molecular rotors [8]. In other aspects, quantum diffusion is revelent for understanding the conductivity of electronics [9], spin transport [10,11], energy transport [12], as well as information scrambling [13,14], and thus has been a subject of intense study in various areas of physics. A landmark of the study on quantum diffusion is the Anderson localization (AL) of electrons in disordered potential [9,15]. Its analog in momentum space is the dynamical localization (DL) in the quantum kicked rotor (QKR), which is a paradigmatic model of Floquet systems [16,17]. The QKR model with incommensurable frequency can mimic the Anderson model in two-dimensional (2D) or three-dimensional (3D) disordered lattice, and is very convenient for theoretical investigation and experimental realization [18–21].

Nowadays, the QKR and its variants have been accepted as ideal systems for exploring rich physics, for instance, Floquet-topological phase [22–26], dynamical phase transition [27], and quantum walk in momentum-space lattice [28–30]. More recently, the study of the $\mathcal{PT}$-symmetric extension of the kicked rotor (PTKR) shows the spontaneous $\mathcal{PT}$-symmetry breaking characterized by the emergence of

the complex quasienergies of the Floquet operators [31,32]. Interestingly, the $\mathcal{PT}$-symmetric kicking potential leads to quantized acceleration of momentum current [33,34] and quantized response of out-of-time ordered correlators [35] in QKR model. The non-Hermiticity of Hamiltonians is now widely accepted as a fundamental modification for the conventional quantum mechanics [36–38]. It is known that open systems which exchange particles or energy with environment can be described by non-Hermitian Hamiltonians [39–41]—for instance, ultracold atoms in dissipative optical lattice, optical wave propagation in lossy media, and electrical circuits with virtual absorption, just to name a few.

Quantum transport in non-Hermitian many-body systems has received intensive investigation [42,43], where the fate of directed current (DC) and DL under the effects of interparticle coupling is still an open issue [44–52]. It is found that in a system of coupled QKRs, the non-Hermitian driving potential can protect the DL, which otherwise is destroyed by interparticle coupling in the Hermitian case [53]. In this paper, we investigate thoroughly the effects of interparticle coupling on quantum transport via a non-Hermitian system of coupled PTKRs. Interestingly, we find the emergence of spontaneous $\mathcal{PT}$-symmetry breaking when the imaginary part of the complex kicking potential is beyond a threshold value which can be effectively modulated by the coupling strength. In the regime of $\mathcal{PT}$-symmetry breaking, the DC in momentum space emerges, and more interestingly, there are two different kinds of energy diffusion: one is ballistic diffusion, and another is modified ballistic diffusion (MBD). The coexistence of DC and MBD is an intrinsic phenomenon in coupled non-Hermitian systems. We further numerically obtain the growth rates of DC and MBD in time for a wide regime of system parameters, which is helpful to guide the Floquet engineering of transport in momentum-space lattice [54,55].

---
*wlzhao@jxust.edu.cn
†jliu@gscaep.ac.cn

Our investigation suggests that the coexistence of DC and MBD results from the intrinsic decoherence effects in non-Hermitian chaotic systems. We also investigate interparticle entanglement due to the interplay between coupling and non-Hermitian parameters.

The paper is organized as follows. In Sec. II, we describe the system. In Sec. III, we show the transport behaviors in our system with an emphasis on the coexistence of the DL and MBD. A summary is presented in Sec. IV.

II. MODEL

The Hamiltonian of the coupled PTKRs reads

$$H = H_1 + H_2 + H_I, \qquad (1)$$

with H_j ($j = 1, 2$) of the individual particle

$$H_j = \frac{p_j^2}{2} + V(\theta_j) \sum_{n=0}^{\infty} \delta(t - t_n), \qquad (2)$$

and the interparticle coupling

$$H_I = \varepsilon \cos(\theta_1 - \theta_2) \sum_{n=0}^{\infty} \delta(t - t_n). \qquad (3)$$

Here, our consideration of the temporal delta modulation of the coupling is just for the convenience of numerical simulation. This kind of coupling has been widely used in previous investigations [49,56]. In our system, the kicking potential is $\mathcal{PT}$ symmetric, i.e., $V(\theta_j) = K[\cos(\theta_j) + i\lambda \sin(\theta_j)]$, with K being the kick strength while λ controls the strength of the imaginary part of $V(\theta_j)$. The $p_j = -i\hbar_{\text{eff}}\partial/\partial\theta_j$ is the angular momentum operator and θ_j is the angle coordinate of each subsystem. The $\hbar_{\text{eff}}$ indicates the effective Planck constant, and the parameter ε is the coupling strength. The time $t_n(= 0, 1, \dots)$ is an integer indicating the number of kicks. All variables are properly scaled and thus in dimensionless units.

The eigenequation of p_j has the expression $p_j|\phi_m^j\rangle = p_m^j|\phi_m^j\rangle$, with $p_m^j = m\hbar_{\text{eff}}$ and $\langle\theta_j|\phi_m^j\rangle = e^{im\theta_j}/\sqrt{2\pi}$. On the basis of the product states $|\phi_m^1, \phi_n^2\rangle = |\phi_m^1\rangle \otimes |\phi_n^2\rangle$, an arbitrary quantum state $|\psi\rangle$ can be expanded as $|\psi\rangle = \sum_{m,n} \psi_{m,n}|\phi_m^1, \phi_n^2\rangle$. One period evolution of the quantum state from t_n to t_{n+1} is given by $|\psi(t_{n+1})\rangle = U|\psi(t_n)\rangle$. The Floquet operator U can be separated into two fractions,

$$U = U_f U_K, \qquad (4)$$

where the free evolution operator of the kinetic term takes the form

$$U_f = \exp\left(-\frac{i}{\hbar_{\text{eff}}} \sum_{j=1}^{2} \frac{p_j^2}{2}\right), \qquad (5)$$

and the evolution operator of the kicking term is

$$U_K = \exp\left\{-\frac{i}{\hbar_{\text{eff}}}\left[\sum_{j=1}^{2} V(\theta_j) + \varepsilon \cos(\theta_1 - \theta_2)\right]\right\}. \qquad (6)$$
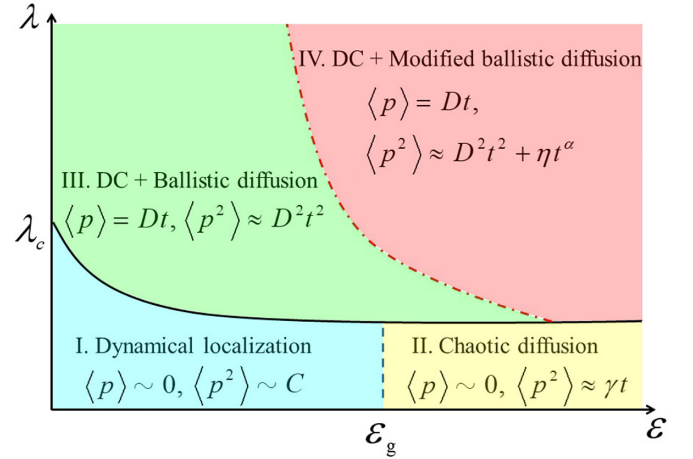
FIG. 1. Schematic diagram for DC and quantum diffusion in the parameter space (λ, ε). The solid curve of λ_c is the boundary of the spontaneous $\mathcal{PT}$-symmetry breaking. Both the dashed and dashed-dotted lines indicate nonsingular crossover between different diffusion phenomena. Here ε_g denotes the threshold value of coupling strength for the crossover from phase I to phase II. It is slightly dependent on λ.

In our investigations, the initial state is set to be the product of the ground states, i.e., $|\psi(t_0)\rangle = |\phi_0^1, \phi_0^2\rangle$.

Numerical simulation for one period evolution splits into two steps, namely, the free evolution and the kicking evolution. The kicking evolution is evaluated in angle coordinate space, i.e., $\langle\theta_1, \theta_2|\psi'\rangle = U_K(\theta_1, \theta_2)\langle\theta_1, \theta_2|\psi(t_j)\rangle$. Then, the fast Fourier transform is exploited to change the state $|\psi'\rangle$ to angular momentum space, yielding its component $\psi'_{m,n}$ in the eigenstate $|\phi_m^1, \phi_n^2\rangle$. Finally, one can conduct the free evolution in angular momentum space, i.e., $\psi_{m,n}(t_{j+1}) = U_f(p_m, p_n)\psi'_{m,n}$. With such a high-efficiency method, one can get the quantum state at arbitrary time [16–19].

We make thorough investigations on the effects of interplay between the non-Hermiticity (i.e., λ) and interparticle coupling (i.e., ε) on the quantum transport behavior with addressing mean current $\langle p \rangle$ and energy diffusion $\langle p^2 \rangle$. As the two particles are identical, we concentrate on the dynamics of one of the particles (say, particle 1), for which $\langle p_1 \rangle = \text{Tr}(\rho_1 p_1)$ and $\langle p_1^2 \rangle = \text{Tr}(\rho_1 p_1^2)$. Here, the reduced density matrix of particle 1, i.e., $\rho_1 = \frac{1}{\mathcal{N}}\text{Tr}_2(|\psi\rangle\langle\psi|)$, is evaluated by tracing out the other degree of freedom from the density matrix of the total system $\rho = |\psi\rangle\langle\psi|$ with $\mathcal{N}$ being the norm of quantum state. Hereafter, we drop the subindex "1" in $\langle p_1 \rangle$ and $\langle p_1^2 \rangle$ for brevity.

The general phase diagram has been investigated and demonstrated schematically by Fig. 1. It is known that, in the unbroken phase of $\mathcal{PT}$ symmetry, i.e., $\lambda < \lambda_c$, there are two different classes of transport behaviors without DC, i.e., $\langle p \rangle \sim 0$, analogous to that of Hermitian systems [57]. Phase I at $\varepsilon < \varepsilon_g$ displays DL with $\langle p^2 \rangle \sim C$, while phase II at $\varepsilon > \varepsilon_g$ demonstrates the chaotic diffusion with $\langle p^2 \rangle \approx \gamma t$. These two classes of energy diffusions are essentially similar to the coupling-induced quantum-classical transition in Hermitian systems [50,58,59]. Here, ε_g denotes the critical value of coupling strength for the nonsingular crossover between the
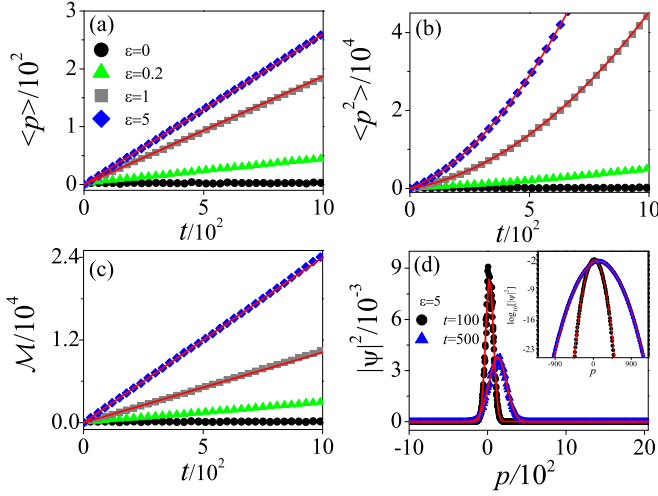
FIG. 2. Time evolution of $\langle p \rangle$ (a), $\langle p^2 \rangle$ (b), and $\mathcal{M}$ (c) with $\varepsilon = 0$ (circles), 0.2 (triangles), 1 (squares), and 5 (diamonds). Red lines in (a), (b), and (c) indicate $\langle p \rangle = Dt$ in Eq. (7), $\langle p^2 \rangle \approx D^2t^2 + \eta t^\alpha$ in Eq. (8), and $\mathcal{M} = \eta t^\alpha$ in Eq. (9) with $\alpha = 1$. (d) Momentum distributions $|\psi(p)|^2$ at time $t = 100$ (circles) and 500 (triangles) for $\varepsilon = 5$. Red lines indicate the fitting functions of the Gaussian form $|\psi(p)|^2 \propto e^{-(p-p_c)^2/\sigma}$. Inset: Same as in the main plot but on a logarithmic y scale. The parameters are $K = 5$, $\hbar_{\text{eff}} = 1$, and $\lambda = 0.01$.

two different classes. We find that it is slightly dependent on the non-Hermitian parameter λ.

There are two additional phases in the regime of $\mathcal{PT}$-symmetry breaking, i.e., $\lambda > \lambda_c$. In phase III, the system displays the DC $\langle p \rangle = Dt$ and ballistic diffusion $\langle p^2 \rangle \approx D^2t^2$, in which the quantum state in momentum space moves unidirectionally while keeping almost a constant wave packet's width. It is similar to that of the PTKR system for a single particle [33–35]. However, with increasing the interparticle coupling further, we find a striking energy diffusion behavior, termed as MBD, in which $\langle p^2 \rangle \approx D^2t^2 + \eta t^\alpha$ with $\alpha < 2$. To our knowledge, this kind of energy diffusion behavior has not been reported before. It unveils the interparticle coupling induced quantum fluctuation effects on the well-known ballistic energy diffusion. Our finding of the coexistence of DC and MBD in phase IV thus completes the phase diagram of quantum diffusions in non-Hermitian coupled systems.

III. DIRECTED CURRENT AND ENERGY DIFFUSION

A. Time evolution of $\langle p \rangle$, $\langle p^2 \rangle$, and $\mathcal{M}$

In the regime of the unbroken phase of $\mathcal{PT}$ symmetry with a real spectrum of quasienergies, the transport behavior of this system has no essential differences from that of the Hermitian case. In our numerical investigations, we choose very small λ, so the $\mathcal{PT}$-symmetry breaking does not occur with $\varepsilon = 0$. Indeed, our numerical results with $\varepsilon = 0$ show that there is neither momentum current, i.e., $\langle p \rangle \sim 0$ [see Fig. 2(a)], nor energy diffusion, i.e., $\langle p^2 \rangle \sim C$ [see Fig. 2(b)], correspondingly the width of the wave packet $\mathcal{M} = \langle p^2 \rangle - (\langle p \rangle)^2 \sim C$ [see Fig. 2(c)], which is clear evidence of the appearance of DL.

In the regime of the $\mathcal{PT}$-symmetry breaking, the system exhibits exotic transport behaviors. We find that the mean value $\langle p \rangle$ increases linearly with time,

$$\langle p \rangle = Dt, \tag{7}$$

which demonstrates the emergence of DC [e.g., $\varepsilon = 1$ in Fig. 2(a)]. Meanwhile, the energy diffusion increases in a way of MBD [e.g., $\varepsilon = 1$ in Fig. 2(b)],

$$\langle p^2 \rangle \approx D^2t^2 + \eta t^\alpha \quad \text{with} \quad \alpha < 2. \tag{8}$$

The corresponding width of the time-evolved wave packet grows as

$$\mathcal{M} = \eta t^\alpha, \tag{9}$$

indicating the fact that unbounded spreading of the wave packet occurs [e.g., $\varepsilon = 1$ in Fig. 2(c)]. Our results, therefore, present solid evidence of the coexistence of DC and MBD due to the interplay between non-Hermitian driving and coupling. After extensive investigations on the energy diffusion for different λ, we find that α varies with λ, which demonstrates the influences of the non-Hermitian driven potential on the energy diffusion.

The probability density distributions of particle 1 in momentum space are shown in Fig. 2(d). One can see that the momentum distribution can be well described by the Gaussian function, i.e., $|\psi(p, t)|^2 \propto e^{-[p-p_c(t)]^2/\sigma(t)}$. Interestingly, the center $p_c(t)$ of the Gaussian wave packet increases with time, which reveals the emergence of the DC in momentum space. Moreover, its width $\sigma(t)$ also increases with time, corresponding to the unbound growth of $\mathcal{M}(t)$. The appearance of Gaussian distribution is usually regarded as a signature of the loss of quantum coherence [48,58] which results in the exponentially localized quantum states, namely, a character of DL [16,17,19], in momentum space. Previous investigations on Hermitian systems have reported that the coupling induces the spreading of the Gaussian wave packet with time, while its center p_c is fixed, thus no DC. Our finding of the coexistence of the increase of both σ and p_c is an unusual kind transport phenomenon due to the quantum decoherence effects in non-Hermitian chaotic systems.

We further numerically investigate the directed transport and energy diffusion for different λ when the coupling ε is sufficiently strong so that the $\mathcal{PT}$-symmetry phase breaking easily emerges for very small λ. Figure 3(a) shows that the momentum current linearly increases with time, i.e., $\langle p \rangle = Dt$. Meanwhile, the energy diffuses in a kind of MBD $\langle p^2 \rangle \approx D^2t^2 + \eta t^\alpha$, for which both η and α vary with λ [see Fig. 3(b)]. Correspondingly, the width of the wave packet increases unboundedly $\mathcal{M} = \eta t^\alpha$ [see Fig. 3(c)]. The momentum distributions are shown in Fig. 3(d). One can see that for weak non-Hermitian driving [e.g., $\lambda \leqslant 1$ in Fig. 3(d)] the momentum distribution can be well described by the Gaussian function. However, for sufficiently large λ [e.g., $\lambda = 5$ in Fig. 3(d)], the quantum state is clearly different from the Gaussian wave packet with irregular distribution in momentum space. It is reasonable to believe that the interplay between non-Hermiticity and coupling dramatically affects
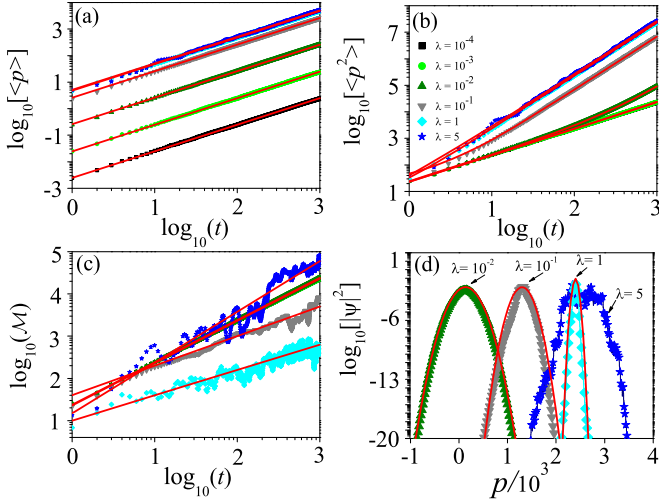
FIG. 3. Time dependence of $\langle p \rangle$ (a), $\langle p^2 \rangle$ (b), and $\mathcal{M}$ (c) for $\varepsilon = 5$ with $\lambda = 10^{-4}$ (squares), 10^{-3} (circles), 0.01 (up triangles), 0.1 (down triangles), 1 (diamonds), and 5 (pentagrams). Red lines in (a), (b), and (c) indicate $\langle p \rangle = Dt$ in Eq. (7), $\langle p^2 \rangle \approx D^2 t^2 + \eta t^\alpha$ in Eq. (8), and $\mathcal{M} = \eta t^\alpha$ in Eq. (9) with $\alpha < 2$. (d) Momentum distributions $|\psi(p)|^2$ for $t = 500$ and $\varepsilon = 5$ with $\lambda = 0.01$ (up triangles), $\lambda = 0.1$ (down triangles), $\lambda = 1$ (diamonds), and $\lambda = 5$ (pentagrams). Red lines indicate the fitting function of the Gaussian form $|\psi(p)|^2 \propto e^{-(p-p_c)^2/\sigma}$. Other parameters are the same as in Fig. 2.

the decoherence effects, which leads to the irregular form of the momentum distribution.

B. Growth rate of $\langle p \rangle$ and $\mathcal{M}$

The growth rates of the momentum current and the width of quantum state are separately defined by $D = \langle p(t_f) \rangle / t_f$ and $\eta = \mathcal{M}(t_f)/t_f^\alpha$. In numerical simulations, the t_f on the scale of hundreds of kicking periods is enough to assure the high precision of numerical results. Figure 4(a) shows that the D increases rapidly from a very small value to saturation with increasing ε. Note that the nonzero value of D for $\varepsilon = 0$ is due to the finite time t_f in numerical calculations. The saturation value of D increases with the increase of λ, which reveals that the acceleration of momentum current is only determined by the non-Hermitian driving with no relation to coupling. As a further step, we numerically investigate the acceleration rate D for various λ. Figure 4(b) shows that the value of D increases linearly with λ, i.e., $D \propto \lambda$, up to saturation. Moreover, the D is almost not dependent on the variation of ε if the coupling strength is strong enough. The growth rate η of the $\mathcal{M}$ for a wide regime of ε and λ is shown in Fig. 4(c). One can find that the η exponentially increases with ε, but without dependence on the variation of λ. Therefore, the spreading of the wave packet in momentum space is mainly determined by the interparticle coupling. Since the MBD $\langle p^2 \rangle \approx D^2 t^2 + \eta t^\alpha$ has two parts, it is clear that the first part of quadratic growth originates from the non-Hermitian driving, while the second part, i.e., ηt^α, is dominated by the competition between coupling and non-Hermitian driving potential. Accordingly, this opens an opportunity for the experimental engineering of the transport behaviors in momentum-space lattice [28–30].
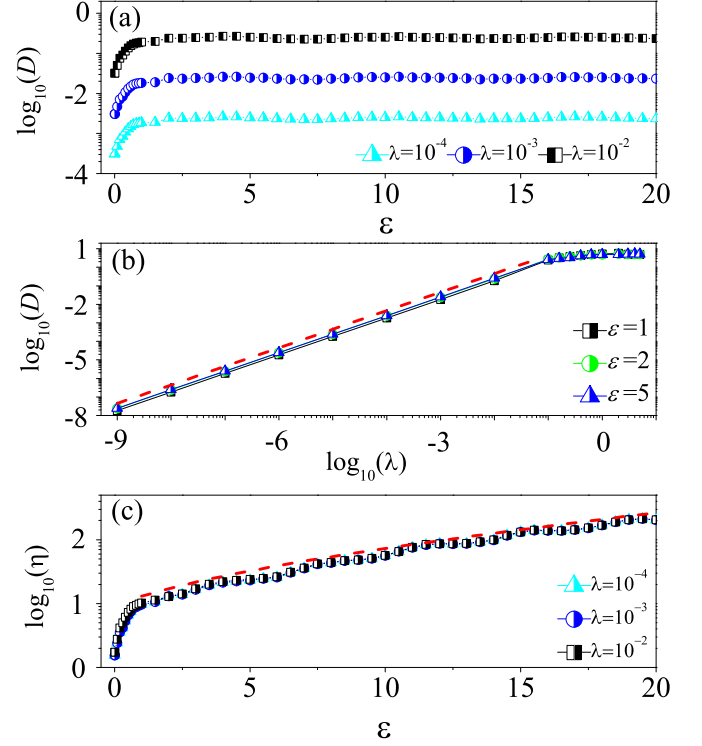
FIG. 4. (a) Growth rate D versus ε with $\lambda = 10^{-4}$ (triangles), $\lambda = 10^{-3}$ (circles), and $\lambda = 10^{-2}$ (squares). (b) The value of D versus λ for $\varepsilon = 1$ (squares), 2 (circles), and 5 (triangles). Red dashed line indicates the fitting function of the form $D \propto \lambda$. (c) Dependence of η on ε with $\lambda = 10^{-4}$ (triangles), $\lambda = 10^{-3}$ (circles), and $\lambda = 10^{-2}$ (squares). Red dashed line indicates the exponential fitting, i.e., $\eta \propto e^{\beta\varepsilon}$ with $\beta = 0.1$. Other parameters are the same as in Fig. 2.

C. Spontaneous $\mathcal{PT}$-symmetry breaking

It is known that without interaction (i.e., $\varepsilon = 0$) there is a threshold value for the imaginary part of the kicking potential, i.e., λ_c, beyond which the system is in the regime of the $\mathcal{PT}$-symmetry breaking phase. For convenience, the norm $\mathcal{N}(t_n) = \sum_{m,n} |\psi_{m,n}(t_n)|^2$ [60–62] is applied to quantify the $\mathcal{PT}$-symmetry phase transition. Figure 5(a) shows
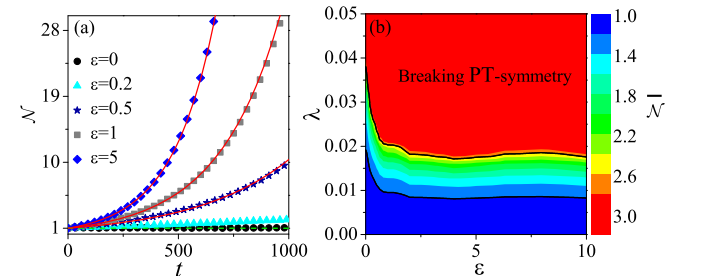
FIG. 5. (a) Norm $\mathcal{N}$ versus time with $\lambda = 0.01$ for $\varepsilon = 0$ (circles), 0.2 (triangles), 0.5 (pentagrams), 1 (squares), and 5 (diamonds). Red solid lines indicate the fitting function of the form $\mathcal{N} = e^{\gamma t}$ with $\gamma = 0.0023$, 0.0035, and 0.0051 for $\varepsilon = 0.5$, 1, and 5, respectively. Green dashed line marks $\mathcal{N} = 1$. (b) The time-averaged value of norm $\bar{\mathcal{N}}$ in the parameter space (λ, ε). The red (blue) area indicates the breaking (unbreaking) phase of $\mathcal{PT}$-symmetry. Other parameters are the same as in Fig. 2.

that, for $\varepsilon = 0$, the $\mathcal{N}$ remains at unity as time evolves, which demonstrates the maintenance of the $\mathcal{PT}$-symmetry phase. It is interesting that, for a nonzero value of ε (e.g., $\varepsilon = 0.2$), the norm increases with time. Exponential growth of the norm, i.e., $\mathcal{N}(t) \propto e^{\gamma t}$, arises for sufficiently strong coupling (e.g., $\varepsilon = 1$), which is solid evidence of the spontaneous $\mathcal{PT}$-symmetry breaking. Therefore, the interparticle coupling dramatically alters the phase transition point λ_c. To investigate the dependence of λ_c on ε, we numerically calculate the time-averaged value of norm $\bar{\mathcal{N}} = (1/t_M) \sum_{n=1}^{M} \mathcal{N}(t_n)$ in the parameter space (λ, ε). Figure 5(b) shows that there are clearly two different regimes, corresponding to $\bar{\mathcal{N}} > 1$ and $\bar{\mathcal{N}} = 1$, respectively. Detailed observations show that the phase transition point λ_c decreases with the increase of ε, which reveals the fact that the interaction is helpful to assist breaking the $\mathcal{PT}$-symmetry phase. By comparison with Fig. 1, one can find that classes III and IV of quantum transport are in the region of the breaking phase of $\mathcal{PT}$ symmetry.

D. Time evolution of the linear entropy

In the decoherence theory, the unavoidable coupling between system and environment leads to the formation of entanglement. After tracing out the degree of freedoms of the environment, the quantum coherence in the state of the system is destroyed, resulting in a mixed state [63,64]. To quantify entanglement, we numerically investigate the time evolution of the linear entropy $S = 1 - \text{Tr}(\rho_1^2)$ [65–67]. Figure 6(a) shows that, for a specific ε (e.g., $\varepsilon = 0.2$), the S increases monotonically with time until saturation, which demonstrates the formation of entanglement. The saturation value of S increases with ε up to the maximum value $S_{\max} \approx 1$, representing the growth of entanglement with coupling strength. Furthermore, we numerically calculate the time-averaged value of the linear entropy, i.e., $\bar{S} = (1/t_M) \sum_{n=1}^{M} S(t_n)$, for a wide regime of ε and λ. Figure 6(c) shows that for a specific λ the $\bar{S}$ increases from zero to almost unity with the increase of ε, which is a solid confirmation of the enhancement of entanglement by coupling.

We further investigate the time evolution of the linear entropy S for a wide regime of λ. Figure 6(b) shows that for small λ (e.g., $\lambda \leqslant 0.1$) the S increases very rapidly from zero to the saturation of almost unity, demonstrating the growth of entanglement in the coupled PTKRs. In this situation, the momentum distribution can be well described by the Gaussian function [see Fig. 3(d)], which is a character of the onset of the decoherence effects. Interestingly, the saturation value of S decreases with the increase of λ. For instance, the saturation of S with $\lambda = 5$ fluctuates around 0.5 as time evolves. The corresponding wave packet differs clearly from the Gaussian function [see Fig. 3(d)], which may imply that the quantum coherence is partially protected by non-Hermitian driving. For sufficiently large λ (e.g., $\lambda = 10$), the S remains almost at zero with time evolution, which is clear evidence of the disentanglement of the two particles due to the effects of the non-Hermitian driving [53,68]. It is reasonable to believe that the loss of quantum coherence is dramatically affected by the interplay between coupling and non-Hermitian driven potential. This sheds light on the issue of the quantum-classical
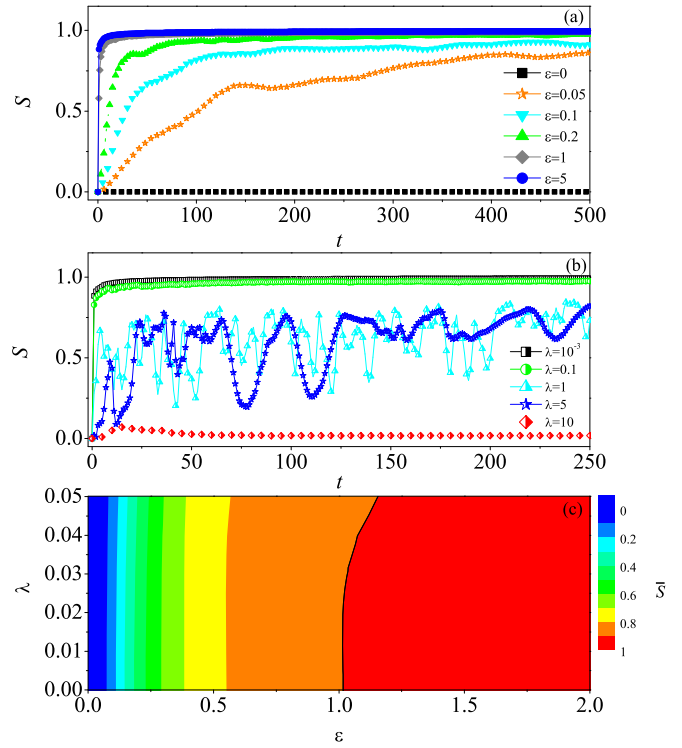
FIG. 6. (a) Linear entropy S versus time for $\lambda = 0.01$ with $\varepsilon = 0$ (squares), 0.05 (pentagrams), 0.1 (down triangles), 0.2 (up triangles), 1 (diamonds), and 5 (circles). (b) Time dependence of S for $\varepsilon = 5$ with $\lambda = 10^{-3}$ (squares), $\lambda = 0.1$ (circles), $\lambda = 1$ (triangles), $\lambda = 5$ (pentagrams), and $\lambda = 10$ (diamonds). (c) Phase diagram of decoherence quantified by the time-averaged $\bar{S}$ in the parameter space (λ, ε). Other parameters are the same as in Fig. 2.

transition induced by quantum decoherence effects in non-Hermitian chaotic systems.

IV. CONCLUSION AND DISCUSSION

In this work, we thoroughly study the quantum transport behaviors in a non-Hermitian PTKR system with interparticle coupling. We find unusual phases of quantum transport, i.e., the coexistence of directed momentum current and ballistic energy diffusion in the regime of $\mathcal{PT}$-symmetry breaking. In particular, in the regime of strong interparticle coupling, we find that quantum fluctuation leads to a modified ballistic diffusion of energy, in which the wave packet's width increases with time in the power laws. Our investigations suggest that the decoherence effect induced by the interplay between the interparticle coupling and the non-Hermitian potential results in these particular transport behaviors. In recent years, the Floquet-driven systems [22,23] with periodical potential in time domain provide ideal platforms for investigating novel phenomena, such as quantum thermalization [69–71], many-body quantum chaos [72–75], and topologically protected transport [76–78]. The fate of DL and AL under the effects of interaction has received extensive investigation in the fields of quantum chaos and condensed matter physics. It is shown that temporally periodical-modulated nonlinearity even induces exponentially fast diffusion in momentum space [79–81]. Our above finding of the coexistence of DC and MBD in coupled

PTKRs serves as an intrinsic element of quantum transport in non-Hermitian systems [82–84].

Our theoretical findings are expected to be observed in the current atomic-optics experiments. Coupled Hermitian kicked rotors have been experimentally realized by subjecting ultracold atoms to two periodically pulsed, incommensurate optical lattices [58], which observes the quantum-classical transition of energy diffusion. The ultracold atoms have a ground state with eigenenergy E_1 and an exited state of hyperfine energy levels E_2^+ and E_2^-. By introducing a decay channel from the excited state with E_2^+ to an additional energy level E_i, the resonance laser gives rise to a strong decay from excited state E_2^+ to E_i, which mimics the non-Hermitian effects [85]. Meanwhile, the standing wave of the off-resonance laser provides the dipole force on the atoms, hence playing the role of the real part of the complex potential. Interestingly, $\mathcal{PT}$-symmetric driven potential can be realized by tuning the relative phase between the off-resonance and resonance standard wave. Therefore, our system is within the research of the state-of-art experiments of atomic-optics.

[1] N. R. Cooper, J. Dalibard, and I. B. Spielman, Rev. Mod. Phys. **91**, 015005 (2019).

[2] J. Wang, G. Casati, and G. Benenti, Phys. Rev. Lett. **124**, 110607 (2020).

[3] L. Wang, G. Benenti, G. Casati, and B. Li, Phys. Rev. Lett. **99**, 244101 (2007).

[4] J. A. Fornés, *Principles of Brownian and Molecular Motors* (Springer, Berlin, 2021).

[5] A. V. Arzola, M. Villasante-Barahona, K. Volke-Sepúlveda, P. Jákl, and P. Zemánek, Phys. Rev. Lett. **118**, 138002 (2017).

[6] B. Lau and O. Kedem, J. Chem. Phys. **152**, 200901 (2020).

[7] T. Sogabe, C. Y. Hung, R. Tamaki, S. Tomić, K. Yamaguchi, N. E. Daukes, and Y. Okada, Commun. Phys. **4**, 38 (2021).

[8] S. Denisov, S. Flach, and P. Hänggi, Phys. Rep. **538**, 77 (2014), and references therein.

[9] P. W. Anderson, Phys. Rev. **109**, 1492 (1958).

[10] J. De Nardis, S. Gopalakrishnan, R. Vasseur, and B. Ware, Phys. Rev. Lett. **127**, 057201 (2021).

[11] M. Ljubotina, L. Zadnik, and T. Prosen, Phys. Rev. Lett. **122**, 150605 (2019).

[12] C. Uchiyama, W. J. Munro, and K. Nemoto, npj Quantum Inf. **4**, 33 (2018).

[13] S. Moudgalya, T. Devakul, C. W. von Keyserlingk, and S. L. Sondhi, Phys. Rev. B **99**, 094312 (2019).

[14] R. J. Lewis-Swan, A. S. Naini, J. J. Bollinger, and A. M. Rey, Nat. Commun. **10**, 1581 (2019).

[15] A. Lagendijk, B. V. Tiggelen, and D. Wiersma, Phys. Today **62**, 24 (2009).

[16] G. Casati, B. V. Chirikov, F. M. Izrailev, and J. Ford, *Stochastic Behavior in Classical and Quantum Hamiltonian Systems*, edited by G. Casati and J. Ford, Lecture Notes in Physics (Springer, Berlin, 1979), Vol. 93.

[17] S. Fishman, D. R. Grempel, and R. E. Prange, Phys. Rev. Lett. **49**, 509 (1982).

[18] D. L. Shepelyansky, Physica D **8**, 208 (1983).

[19] G. Casati, I. Guarneri, and D. L. Shepelyansky, Phys. Rev. Lett. **62**, 345 (1989).

[20] J. Chabé, G. Lemarié, B. Grémaud, D. Delande, P. Szriftgiser, and J. C. Garreau, Phys. Rev. Lett. **101**, 255702 (2008).

[21] G. Lemarié, J. Chabé, P. Szriftgiser, J. C. Garreau, B. Grémaud, and D. Delande, Phys. Rev. A **80**, 043626 (2009).

[22] J. H. Shirley, Phys. Rev. **138**, B979 (1965).

[23] M. Bukov, L. D'Alessio, and A. Polkovnikov, Adv. Phys. **64**, 139 (2015).

[24] D. Y. H. Ho and J. B. Gong, Phys. Rev. Lett. **109**, 010601 (2012).

[25] Y. Chen and C. S. Tian, Phys. Rev. Lett. **113**, 216802 (2014).

[26] L. W. Zhou and J. B. Gong, Phys. Rev. A **97**, 063603 (2018).

[27] C. Hainaut, P. Fang, A. Rançon, J. F. Clément, P. Szriftgiser, J. C. Garreau, C. S. Tian, and R. Chicireanu, Phys. Rev. Lett. **121**, 134101 (2018).

[28] S. Dadras, A. Gresch, C. Groiseau, S. Wimberger, and G. S. Summy, Phys. Rev. Lett. **121**, 070402 (2018).

[29] S. Dadras, A. Gresch, C. Groiseau, S. Wimberger, and G. S. Summy, Phys. Rev. A **99**, 043617 (2019).

[30] D. Z. Xie, T. S. Deng, T. Xiao, W. Gou, T. Chen, W. Yi, and B. Yan, Phys. Rev. Lett. **124**, 050502 (2020).

[31] S. Longhi, Phys. Rev. A **95**, 012125 (2017).

[32] C. T. West, T. Kottos, and T. Prosen, Phys. Rev. Lett. **104**, 054102 (2010).

[33] W. L. Zhao, J. Z. Wang, X. H. Wang, and P. Q. Tong, Phys. Rev. E **99**, 042201 (2019).

[34] W. L. Zhao, P. K. Gong, J. Z. Wang, and Q. Wang, Chinese Phys. B **29**, 120302 (2020).

[35] W. L. Zhao, Phys. Rev. Res. **4**, 023004 (2022).

[36] C. M. Bender and S. Boettcher, Phys. Rev. Lett. **80**, 5243 (1998).

[37] Y. Ashida, Z. P. Gong, and M. Ueda, Adv. Phys. **69**, 249 (2020).

[38] N. Moiseyev, *Non-Hermitian Quantum Mechanics* (Cambridge University, Cambridge, 2011).

[39] H. Ritsch, P. Domokos, F. Brennecke, and T. Esslinger, Rev. Mod. Phys. **85**, 553 (2013).

[40] K. G. Makris, R. El-Ganainy, D. N. Christodoulides, and Z. H. Musslimani, Phys. Rev. Lett. **100**, 103904 (2008).

[41] H. N. Li, A. Mekawy, A. Krasnok, and A. Alù, Phys. Rev. Lett. **124**, 193901 (2020).

[42] T. Eichelkraut, R. Heilmann, S. Weimann, S. Stützer, F. Dreisow, D. N. Christodoulides, S. Nolte, and A. Szameit, Nat. Commun. **4**, 2533 (2013).

[43] Z. H. Xu and S. Chen, Phys. Rev. A **103**, 043325 (2021).

[44] F. Borgonovi, F. M. Izrailev, L. F. Santos, and V. G. Zelevinsky, Phys. Rep. **626**, 1 (2016), and references therein.

[45] S. Lellouch, A. Rançon, S. De Bièvre, D. Delande, and J. C. Garreau, Phys. Rev. A **101**, 043624 (2020).

[46] R. Chicireanu and A. Rançon, Phys. Rev. A **103**, 043314 (2021).

[47] V. Vuatelet and A. Rançon, Phys. Rev. A **104**, 043302 (2021).

[48] D. Rossini, G. Benenti, and G. Casati, Phys. Rev. E **74**, 036209 (2006).

[49] C. Duval, D. Delande, and N. Cherroret, Phys. Rev. A **105**, 033309 (2022).

[50] H. K. Park and S. W. Kim, Phys. Rev. A **67**, 060102(R) (2003).

[51] J. H. See Toh, K. C. McCormick, X. Tang, Y. Su, X. Luo, C. Zhang, and S. Gupta, Nat. Phys. **18**, 1297 (2022).

[52] A. Cao, R. Sajjad, H. Mas, E. Q. Simmons, J. L. Tanlimco, E. Nolasco-Martinez, T. Shimasaki, H. Esat Kondakci, V. Galitski, and D. M. Weld, Nat. Phys. **18**, 1302 (2022).

[53] K. Q. Huang, W. L. Zhao, and Z. Li, Phys. Rev. A **104**, 052405 (2021).

[54] A. C. Keser, S. Ganeshan, G. Refael, and V. Galitski, Phys. Rev. B **94**, 085120 (2016)

[55] C. Hainaut, A. Rançon, J. F. Clément, I. Manai, P. Szriftgiser, D. Delande, J. C. Garreau, and R. Chicireanu, New J. Phys. **21**, 035008 (2019).

[56] E. B. Rozenbaum and V. Galitski, Phys. Rev. B **95**, 064303 (2017).

[57] D. L. Shepelyansky, Phys. Rev. Lett. **73**, 2607 (1994).

[58] B. Gadway, J. Reeves, L. Krinner, and D. Schneble, Phys. Rev. Lett. **110**, 190401 (2013).

[59] S. Adachi, M. Toda, and K. Ikeda, Phys. Rev. Lett. **61**, 659 (1988).

[60] L. W. Zhou, Q. H. Wang, H. L. Wang, and J. B. Gong, Phys. Rev. A **98**, 022129 (2018).

[61] L. W. Zhou and J. B. Gong, Phys. Rev. B **98**, 205417 (2018).

[62] S. Longhi, Phys. Rev. B **103**, 054203 (2021).

[63] W. H. Zurek, Rev. Mod. Phys. **75**, 715 (2003).

[64] M. Schlosshauer, Rev. Mod. Phys. **76**, 1267 (2005).

[65] L. E. C. Rosales-Zárate, and P. D. Drummond, Phys. Rev. A **84**, 042114 (2011).

[66] E. Santos and M. Ferrero, Phys. Rev. A **62**, 024101 (2000).

[67] F. Buscemi, P. Bordone, and A. Bertoni, Phys. Rev. A **75**, 032301 (2007).

[68] K. Q. Huang, W. L. Li, W. L. Zhao, and Z. Li, Chinese Phys. B **31**, 090301 (2022).

[69] C. Fleckenstein and M. Bukov, Phys. Rev. B **103**, L140302 (2021).

[70] S. D. Geraedts, R. Nandkishore, and N. Regnault, Phys. Rev. B **93**, 174202 (2016).

[71] M. Malishava and S. Flach, Phys. Rev. Lett. **128**, 134102 (2022).

[72] C. Rylands, E. B. Rozenbaum, V. Galitski, and R. Konik, Phys. Rev. Lett. **124**, 155302 (2020).

[73] Q. F. Zhao, C. A. Müller, and J. B. Gong, Phys. Rev. E **90**, 022921 (2014).

[74] E. Lundh, Phys. Rev. E **74**, 016212 (2006).

[75] X. Wang, H. R. Li, and F. L. Li, New J. Phys. **22**, 033037 (2020).

[76] R. Roy and F. Harper, Phys. Rev. B **95**, 195128 (2017).

[77] A. Díaz-Fernández, E. Díaz, A. Gómez-León, G. Platero, and F. Domínguez-Adame, Phys. Rev. B **100**, 075412 (2019).

[78] C. B. Dag and A. Mitra, Phys. Rev. B **105**, 245136 (2022).

[79] W. L. Zhao, J. Z. Wang, and W. G. Wang, J. Phys. A: Math. Theor. **52**, 305101 (2019).

[80] W. L. Zhao, L. W. Zhou, J. Liu, P. Q. Tong, and K. Q. Huang, Phys. Rev. A **102**, 062213 (2020).

[81] I. Guarneri, Phys. Rev. E **95**, 032206 (2017).

[82] X. M. Zhao, C. X. Guo, M. L. Yang, H. Wang, W. M. Liu, and S. P. Kou, Phys. Rev. B **104**, 214502 (2021).

[83] Z. F. Yu, J. K. Xue, L. Zhuang, J. Zhao, and W. M. Liu, Phys. Rev. B **104**, 235408 (2021).

[84] X. M. Zhao, C. X. Guo, S. P. Kou, L. Zhuang, and W. M. Liu, Phys. Rev. B **104**, 205131 (2021).

[85] C. Keller, M. K. Oberthaler, R. Abfalterer, S. Bernet, J. Schmiedmayer, and A. Zeilinger, Phys. Rev. Lett. **79**, 3327 (1997).